# MERGING AN ANALYTICAL AERODYNAMIC MODEL FOR HELICOPTER APPLICATIONS WITH A STATE-SPACE FORMULATION FOR UNSTEADY AIRFOIL BEHAVIOR

Maximilian Mindt
Maximilian.Mindt@dlr.de
German Aerospace Center (DLR), Institute of Flight Systems
Lilienthalplatz 7, 38108 Braunschweig, Germany

## ABSTRACT

A new comprehensive simulation tool for computation of the whole helicopter is currently being developed at the Institute of Flight Systems of DLR. A main requirement of such a tool is the calculation of the aerodynamic forces acting at the blades, including all effects that are typical for helicopter rotor operational conditions, while maintaining small calculation times. Therefore, for the calculation of the rotor blade element aerodynamics, a semi-empirical analytical model is used. A formulation in state-space description was chosen to represent the unsteady circulation lag and the modeling of the noncirculatory force response was also added. The analytical models' formulation of the unsteady viscous effects, i.e. stall delay, was transferred to state-space form as well. The resulting combined model is used for the calculation of steady airfoil data as well as unsteady hysteresis curves for a harmonically oscillating airfoil. The results are compared to CFD data.

## NOMENCLATURE

| | |
|---|---|
| $A_n$ | coefficients of indicial functions |
| $b_n$ | exponents of indicial functions |
| $C$ | aerodynamic coefficient |
| $C_{L_\alpha}$ | lift curve slope |
| $Ma$ | Mach number |
| $K$ | noncirculatory time constant function |
| $T$ | time constant, $s$ |
| $V$ | velocity, $m/s$ |
| $a$ | speed of sound, $m/s$ |
| $c$ | chord length, $m$ |
| $k$ | reduced frequency |
| $l$ | section lift, $N/m$ |
| $q$ | dynamic pressure, $N/m^2$ |
| $s$ | generalized time variable |
| $t$ | time, $s$ |
| $x$ | state variable |
| $\alpha$ | angle of attack, $deg$ |
| $\beta$ | Prandtl-Glauert compressibility correction |
| $\Gamma$ | circulation function |
| $\Delta$ | difference |
| $\rho$ | air density, $kg/m^3$ |
| $\phi$ | indicial response function |
| $\omega$ | angular frequency, $rad/s$ |

### Indices

| | |
|---|---|
| $D$ | drag |
| $I$ | impulsive |
| $L$ | lift |
| $M$ | moment, aerodynamic coefficient |
| $N$ | normal |
| $att$ | attached |
| $b$ | bubble |
| $c$ | circulatory |
| $det$ | detached |
| $eff$ | effective |
| $geom$ | geometric |
| $m$ | moment, based on sonic pressure |
| $nc$ | noncirculatory |
| $os$ | stall overshoot |
| $sc$ | sub-critical |
| $spc$ | supercritical |
| $ss$ | steady stall |
| $x$ | in chord direction |
| $z$ | perpendicular to chord |
| $+, -$ | positive, negative direction |

## 1. INTRODUCTION

The Institute of Flight Systems of the German Aerospace Center has long-standing experience regarding the simulation of isolated helicopter rotors. The simulation tool S4 was developed in-house and extensive validation of this tool has been conducted ever since, for example using the results of the HART II test campaign [1]. Even though S4 serves as a useful device for the preparation of wind tunnel tests, this tool exhibits major limitations in its simulation capabilities. These are for instance the preconditions that the rotor head is fixed in space and only one rotor can be simulated.

Since these essential limitations are hard to overcome with the code already at hand, a new comprehensive simulation tool for computation of the whole helicopter is currently being developed at the Institute. This new code

is called VAST, which stands for **V**ersatile **A**eromechanics **S**imulation **T**ool.

A main requirement of such a tool is the calculation of the aerodynamic forces acting at the blades, including all effects that are typical for helicopter rotor operational conditions, while maintaining small calculation times. In forward flight the velocities due to rotation of the rotor are superposed with the forward flight velocity, which leads to a large variation of Mach number, angle of attack and yaw velocity component in the course of a rotation even under steady flight conditions. Therefore, essential effects to be represented by the model are the influence of compressibility, unsteadiness and yawed flow.

In order to model the aerodynamic response due to arbitrary excitation at low computational cost, the so called indicial functions are commonly used [2]. These give the response in lift and moment resulting from a step change in angle of attack. The actual aerodynamic force time history can then be calculated by superposition and time integration of the different indicial functions. The first solution pertaining to this kind of problem was that of Wagner [3] for the lift response due to a sudden change in angle of attack in incompressible flow. Many derivations have been made for different types of forcing and for the inclusion of effects of compressibility, e.g. the response to an encounter with a sharp-edged gust as described by Küssner [4]. Since the exact formulations are computationally expensive, approximate solutions in the form of exponential functions like that of Jones [5] to the Wagner and Küssner function for wings considering the aspect ratio have been formulated. Mazelsky and Drischler [6] determined numerical solutions for these functions under consideration of compressibility and also stated approximative exponential functions for Mach numbers of 0.5, 0.6 and 0.7.

Beddoes [7] later established a generalization of the indicial lift response by appropriate scaling of the generalized time variable. A comparative study of calculated and experimental unsteady lift responses led to the adaption of the approximate functions for general applicability in [8]. Lomax stated in [2] that the circulatory lift development after penetration of a sharp edged gust equals that of a step change in angle of attack after an initial phase. Based on this finding, Leishman and Beddoes [9] developed a generalized model for the unsteady airfoil behavior presenting noncirculatory (impulsive) indicial responses fitting to the generalized lift indicial functions. In a later work [10], Leishman transferred the previously derived model into state-space formulation.

The model described above was developed for attached flow, but extensions to model flow separation and dynamic stall have been presented in [9]. Several functions are introduced for the incorporation of leading edge and trailing edge stall, mainly on the basis of first order lags. The corresponding time constants have to be identified based on the dynamic behavior of the airfoil. A drawback of the proposed method is that the time constants have to be adapted for different states of the airfoil flow field. The model also does not account for the effect of sweep.

A model that includes the effect of yawed flow conditions and works without the need to switch between different flow conditions throughout the simulation is that developed by Leiss [11]. It is based on superposition of three different force components, namely the force resulting from fully separated flow according to Newton's law, the separated circulatory flow, and the attached circulatory flow. Furthermore, the influence of compressibility and dynamic stall is included in the model. van der Wall [12] proposed some adaption to this model that will be introduced in section 2.3.

In this paper, the usage of the state-space model for the indicial aerodynamics in conjunction with Leiss's adapted aerodynamics model is presented. Discussion of the hysteresis curves for a NACA 23012 airfoil with a tabbed trailing edge experiencing generic unsteady forcing is carried out using data obtained with the CFD code TAU [13] for comparison.

## 2. AERODYNAMIC MODEL

### 2.1. Indicial Response formulation

In this section, the formulation of the indicial response is outlined for the example of a step change in angle of attack $\Delta\alpha$. The analogous representations for moment contributions and the response to pitching of the airfoil can be found in the respective cited publications.

The circulatory indicial response is commonly denoted $\phi_c$ and written in terms of the variable $s$ that represents the distance traveled by the airfoil in half-chord-lengths:

$$s = t\,\frac{V}{c/2} = t\,\frac{2aMa}{c} = t\,\frac{2Ma}{T} \tag{1}$$

where $t$ is the time, $V$ the velocity of the free stream relative to the airfoil, $c$ corresponds to the chord length and $T = c/a$ is a time constant using the speed of sound $a$. In the incompressible case, the circulatory section lift due to a step change in angle of attack can be computed as

$$l(s) = 2\pi\frac{\rho}{2}V^2 c\,\Delta\alpha\,\phi_c(s) \tag{2}$$

with the air density $\rho$. $\phi_c$ was chosen to give a value of unity for very large values of $s$. Dividing the section lift by the dynamic pressure $q = \rho/2\ V^2$ and the chord length, the lift coefficient results. The factor of $2\pi$ is the lift curve slope $C_{L_\alpha}$ for incompressible flat plate aerodynamics. This term can be replaced by the actual lift curve slope for the lift response of the airfoil in use, e.g.

$$C_{L,c}(s) = C_{L_\alpha}\Delta\alpha\,\phi_c(s) \tag{3}$$

For subsonic compressible flow, the development of lift as well as the asymptotic behavior changes and approximate formulations for different Mach numbers exist, like that of Mazelsky and Drischler [6]. Beddoes [7] showed that by scaling $\phi_c$ with the Prandtl-Glauert correction factor $\beta = \sqrt{1 - Ma^2}$, and substituting $s$ in $\phi_c$ by $s\beta^2$, the compressibility effects on the lift transfer function can approximately be represented. By scaling of the indicial response

function, it is possible to use the actual value of $C_{L_\alpha}$ in equation (3) that changes according to the Prandtl-Glauert correction.

The approximate solutions for $\phi_c$ are commonly expressed in the form of two exponential terms, i.e.

$$\begin{aligned}\phi_c(s) &= 1 - A_1\, e^{-b_1 s} - A_2\, e^{-b_2 s} \\ &= 1 - A_1\, e^{-b_1 \frac{2Ma}{T} t} - A_2\, e^{-b_2 \frac{2Ma}{T} t}.\end{aligned} \tag{4}$$

In [8], Beddoes modified the values resulting from numerical calculations slightly to obtain a better fit to experimental data. His final parameter set was $A_1 = 0.3$; $A_2 = 0.7$; $b_1 = 0.14$; $b_2 = 0.53$.

The circulatory response presented before is only one effect of a sudden change in angle of attack. In the instance of the change, an infinite impulsive force results in the incompressible case as well. For compressible flow, the noncirculatory force retains a finite value at the start and then decays. Leishman [14] obtained an approximate value for this decay by matching the gradient of the total response for $s = 0$. The resulting formula for the noncirculatory normal force coefficient $C_{N,nc}$ reads

$$C_{N,nc} = \frac{4\Delta\alpha}{Ma} e^{-(K_\alpha T)^{-1} t} \tag{5}$$

with

$$K_\alpha = \frac{2}{2(1 - Ma) + 2\pi\beta Ma^2 (A_1 b_1 + A_2 b_2)}. \tag{6}$$

This additional time constant function is close to a value of unity in the low Mach number range and shows a strong increase at $Ma > 0.8$.

The impulsive force component is not occurring for an airfoil entering a gust because in this case at the start there is no change in the velocities acting at the airfoil. Hence, for this kind of forcing only the circulatory part is relevant. Lomax [2] established that after an initial time, the indicial response due to gust encounter is the same as that for the step change in $\alpha$. Therefore, the herein described model makes no distinction in the circulatory force for these different types of forcing.

To be able to describe the output of a system at any time, the current state of the system has to be known. The entirety of the state variables is called the state space in control theory and their change over time is dependent on the current state itself and the input of the system. For further information about control theory, the reader is referred to the related literature.

The lift and moment generated by arbitrary forcing can be viewed as the output of the unsteady aerodynamic system, as pointed out by Leishman in [10]. There, he shows the transfer of the indicial response equation into state space form. For the circulatory lift response, the time derivative of the states $x_i$ can be determined to

$$\begin{bmatrix}\dot{x}_1 \\ \dot{x}_2\end{bmatrix} = \frac{2Ma}{T}\beta^2 \begin{bmatrix}-b_1 & 0 \\ 0 & -b_2\end{bmatrix} \begin{bmatrix}x_1 \\ x_2\end{bmatrix} + \begin{bmatrix}1 \\ 1\end{bmatrix} \alpha(t) \tag{7}$$

and the output equation reads

$$C_{L,c}(t) = \frac{2\pi}{\beta}\frac{2Ma}{T}\beta^2 \begin{bmatrix}A_1 b_1 & A_2 b_2\end{bmatrix} \begin{bmatrix}x_1 \\ x_2\end{bmatrix}. \tag{8}$$

For the noncirculatory response, the state space formulation is scalar because only one decay term was introduced:

$$\dot{x}_3 = -\frac{1}{K_\alpha T} x_3 + \alpha(t) \tag{9}$$

$$C_{N,nc} = \frac{4}{Ma}\dot{x}_3 = -\frac{4}{Ma}\frac{1}{K_\alpha T} x_3 + \frac{4}{Ma}\alpha(t) \tag{10}$$

Transferring the response functions for the aerodynamic moment as well and also accounting for pitch rate responses, a total of eight state equations results. The full set of formulae is presented in [10].

### 2.2. Leiss's aerodynamic model

The aerodynamic model proposed by Leiss [11] varies from other typically applied models within the definition of the aerodynamic coefficients. In most applications, the coefficients are expressed in the so-called aerodynamic system, i.e. lift component perpendicular to the flow velocity and drag component in flow direction. Normalization is carried out using the dynamic pressure and the chord, as shown in the transition from equation (2) to equation (3). Furthermore, the chord length is used as additional parameter for normalization of the moment.

For helicopter applications, this leads to problems caused by the varying flow field at the blade elements. In the first place, the aerodynamic coefficients yield no direct measure of the acting forces and moments at different radii and azimuths due to the permanently varying dynamic pressure. A second problem is the occurrence of reversed flow at the retreating blade side. The angle of attack of $180\ deg$ is equivalent to $-180\ deg$ and for dynamic variations around that angle, no smooth transition is possible.

In the Leiss model, in contrast to traditional definitions, the coefficients are expressed perpendicular to and in airfoil direction and are based on the dynamic pressure of the speed of sound. The definitions of the systems are shown in Figure 1. Transformation between the different systems

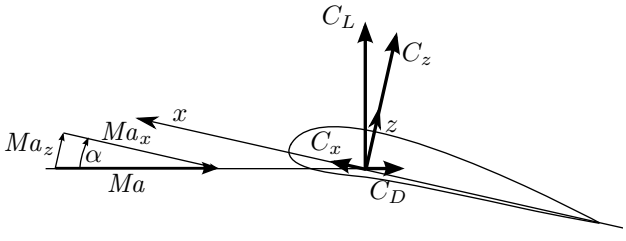


Figure 1: Definition of the force coefficients

can be applied using the following formulae:

$$\begin{aligned}C_z &= Ma_x\ Ma\ C_L + Ma_z\ Ma\ C_D \\ C_x &= Ma_z\ Ma\ C_L - Ma_x\ Ma\ C_D \\ C_m &= Ma^2\ C_M\end{aligned} \tag{11}$$

One benefit of this formulation is that the magnitude of the coefficient now directly corresponds to the acting force. For the application in helicopters this is particularly useful as coefficients at different radial stations and of different time steps can directly be compared. Another advantage of this formulation is that the coefficients are continuous throughout the entire $Ma_x$-$Ma_z$ range including reversed flow and therefore better suited for integration in an analytical model, as visualized in [15].

The aerodynamic model is based on analytical representation of the airfoil properties gained with experimental data by superposition of three physical force sources. Following Leiss, these are resulting from fully separated flow according to Newton's law, the separated circulatory flow, and the attached circulatory flow. The whole set of formulae can be found in [11]. This section focuses on the attached circulatory flow formulation since two main factors of unsteady flow are accounted for there, which is dynamic stall and sweep influence. The formulae shown here pertain to the normal force coefficient and an exemplary division between the different basic flow effects can be seen in Figure 2. It also depicts the additional circulation component due to leading edge bubble burst, denoted by index $b$.

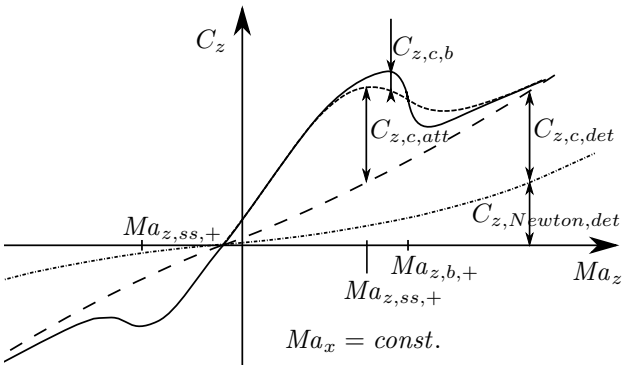


Figure 2: Distinction of force components by mechanism

The circulatory normal force coefficient $C_{z,c}$ is determined using

$$C_{z,c,att,+} = |Ma_x| \frac{dC_{z,+}}{dMa_z}(Ma_x) \times Ma_{z,ss,+}(Ma_x)\Gamma_+(Ma_z, Ma_{z,ss,+}) \quad (12)$$

The index $+$ denotes this is the force component due to positive angle of attack. A respective formulation exists for negative angles of attack circulation. In case it is desired to model the influence - and when there is enough data to substantiate the set up of such a model - similar formulae can be set up for the smaller attached flow regions in rearward flow.

The derivative $dC_{z,+}/dMa_z(Ma_x)$ is comparable to the lift curve slope $C_{L_\alpha}(Ma)$ and similarly depends on the tangential Mach number. For small angles of attack this is practically the same as the Mach number, since $Ma_x = Ma\ cos(\alpha)$. The normal Mach number of steady stall $Ma_{z,ss}$ represents the stall angle of attack where the maximum circulation occurs. This can be seen in the equation for the circulation function $\Gamma$, representing the bell-shaped curve of Figure 2:

$$\Gamma_+ = \frac{c^2_{ss,+}(Ma_x)}{[Ma_z - Ma_{z,ss,+}(Ma_x)]^2 + c^2_{ss,+}(Ma_x)} \quad (13)$$

The parameter $c_{ss}$ is also dependent on $Ma_x$, normalizes the maximum of the circulation to unity and determines the width of the curve. Another circulatory contribution is the generation of a leading edge bubble that delays the occurrence of stall via aiding in the reattachment of the flow behind the bubble. When the bubble bursts this leads to a sharper decrease of lift, though. This effect occurs only at lower Mach numbers. The circulation of the bubble $\Gamma_b$ is determined by

$$\Gamma_{b,+} = c_{b,+} \frac{[Ma_z - Ma_{z,b,+}]Ma^2_{z,b,max,+}}{[Ma_z - Ma_{z,b,+}]^2 + Ma^2_{z,b,max,+}} \quad (14)$$

The normal Mach number of bubble burst $Ma_{z,b}$, that of the maximum circulation $Ma_{z,b,max}$ and the additional coefficient $c_b$ are again dependent on $Ma_x$, but the identifier has been left out in equation (14) to fit it onto the page. For all the Mach number dependent parameters, Leiss proposed polynomial representations in terms of $Ma_x$. Similar equations have to be set up for tangential and moment coefficients.

The influence of sweep is accounted for via a steady stall shift $\Delta Ma_{z,ss}$ that shifts the stall to higher $Ma_z$ numbers for the $+$ circulation curve and to lower $Ma_z$ numbers for the circulation at negative angles of attack, i.e. the sweep aids in keeping the flow attached for larger positive as well as larger negative angles of attack. Leiss postulated a simple quadratic dependence on the radial Mach number $Ma_y$ for this influence in [16]:

$$\Delta Ma_{z,ss,y,+/-} = c_{y_1,+/-}\ Ma_y^2 \quad (15)$$

Furthermore, Leiss deduced a decreasing of the lift curve slope from experimental results he investigated. For this drop, he proposed an additional term of $c_{y2,+/-}\ Ma_y^2$ to be added in the denominator of equation (13).

For the inclusion of circulation lag effects in unsteady motion, Leiss proposed to use the Wagner and Küssner functions in order to determine the change in $Ma_z$ value in relation to the geometrical value. The formulation presented in [15] builds on the precondition of harmonic oscillation, though.

Dynamic stall is accounted for via a shift of the point of stall $Ma_{z,ss}$. Leiss also only showed the solution for harmonic oscillations in [15], but it can be deduced from that solution that the basic formula for the shift is an exponential equation dependent on two overshoot parameters

$$\Delta Ma_{z,ss} = A_{os}\ e^{-b_{os}s} \quad (16)$$

### 2.3. Adaption of the Leiss Model

The model of Leiss presented in the previous section is based on theoretical considerations and deductions from experiments. It was validated with experimental data of the symmetric NACA 0012 airfoil. Between the first publication in 1984 [15] and the final presentation of the model in 1987 [11] still changes regarding the basic formulae are apparent, i.e. the model was still in development. van der Wall [12] published results using this model for the NACA 23012 airfoil and stated that some adaption had been made to the model. These changes will be described in this section.

The first change pertains to the detached circulatory flow. The equation stated by Leiss for the normal force coefficient consists of two parts. A sub-critical term (parameter indices $sc$) starts at a value of $\pi/2$ in incompressible conditions and decreases for higher velocities. The supercritical term (parameter indices $spc$) starts at zero, has its maximum at a Mach number of unity and beyond that decreases approximately according to the rule of Ackeret. The formula reads

$$C_{z,c,det} = \frac{Ma_z Ma_x^2}{Ma}\left(\frac{\pi}{2}\frac{c_{sc}^4}{Ma^4 + c_{sc}^4} + 4\,\frac{Ma^3}{(Ma^2 - c_{spc,max}^2)^2 + c_{spc}^4}\right) \tag{17}$$

The adaption by van der Wall allows for a scaling of the overall behavior via the parameter $c_{det,0}$. Also, a linear variation of the angle-of-attack-dependence with tangential Mach number is possible using $c_{det,1}$:

$$C_{z,c,det} = c_{det,0}\frac{Ma_x^2}{Ma}(Ma_z - c_{det,1}Ma_x) \times \left(\frac{\pi}{2}\frac{c_{sc}^4}{Ma^4 + c_{sc}^4} + 4\,\frac{Ma^3}{(Ma^2 - c_{spc,max}^2)^2 + c_{spc}^4}\right) \tag{18}$$

The same modification was employed for the moment coefficient. As mentioned in section 2.2, Leiss proposed polynomial descriptions for the attached circulatory flow parameters. In the parameter optimizations conducted to set up the model of the NACA 23012 airfoil in [12], it turned out that due to the nonlinear behavior of the parameters this approach was not practicably feasible to account for the actual behavior of the airfoils throughout the whole Mach range. Especially the bubble burst effect that vanishes at higher Mach numbers would lead to difficulties here. Therefore, the parameters are identified for different Mach numbers and an interpolation is carried out inside the parameter data set during calculation.

The bubble circulation equation (14) was changed into a two-term approach

$$\Gamma_b = c_b^2\left(\frac{1}{[Ma_z - Ma_{z,b,max1}]^2 + c_b^2} - \frac{1}{[Ma_z - Ma_{z,b,max2}]^2 + c_b^2}\right) \tag{19}$$

This formulation allows for more localized effects in the representation of the airfoil coefficients. For the incorporation of sweep, a multitude of changes was made. Firstly, the stall shift is formulated dependent on the sweep angle $\gamma$ as

$$\Delta Ma_{z,ss,y} = |Ma_x|\, tan(c_{y_1}\gamma^2) \tag{20}$$

The adaption of the denominator in equation (13) by an additional term for the yawed flow was replaced by a modification of $c_{ss}$, i.e

$$c_{ss,y} = c_{ss} + c_{y_2}\Delta Ma_{z,ss,y} \tag{21}$$

The same approach is used to model the influence of yaw velocity on the bubble burst parameter $c_b$, but using a different parameter $c_{y_3}$. This additional modification of both circulation functions is also implemented for the influence of the unsteady stall shift.

## 3. MERGING OF THE AERODYNAMIC MODELS

Regarding the development of circulatory lift, the indicial response is often seen as a shift from geometric angle of attack $\alpha_{geom}$ to an effective angle of attack $\alpha_{\mathit{eff}}$. This analogy was also stated by Beddoes in [7] for example. The original derivations of Wagner and Küssner are solutions for the induced velocity flow field due to changes in the bound and shed circulation after small disturbances, though. As stated in section 2.2, Leiss proposed to extend the usage of those solutions for the development of $\alpha$ to all changes in incidence angle.

Since the Leiss model works with the velocity components tangential, normal and radial to the chord, it suggests itself to use the effective flow components directly. For the normal velocity component this is a straight-forward approach given the small angle assumption that is underlying the derivation. Looking at the tangential velocity component this comes even closer to the development of the effective angle of attack if the small angle assumption is dropped. This is visualized in Figure 3 where the black solid line shows the development of $\alpha_{\mathit{eff}} = \Delta\alpha\ \phi_c(s)$. The dashed red line gives $\alpha_{\mathit{eff}}$ which is computed by applying the circulatory response to the changes in the Mach number components at the airfoil, i.e. $Ma_{i,\mathit{eff}} = \Delta Ma_i\ \phi_c(s)$ with $i = x, z$, and then computing the angle as $\alpha_{\mathit{eff}} = tan^{-1}(Ma_z/Ma_x)$. The deviation resulting from using the different approaches is shown in Figure 4 to be under one per mill throughout the whole time range. This deviation is solely dependent on the magnitude of the angle of attack change and originates in the nonlinearity of the trigonometric function involved.

In [15], Leiss proposed to use an exponential formulation for the lag in $Ma_{x,\mathit{eff}}$ from changes in the $Ma_x$ velocity component. The parameters for the approximation should be identified using measurements. Based on the considerations of the last paragraph, the usage of the indicial lift response function for the $Ma_{x,\mathit{eff}}$-lag due to angle of attack change seems appropriate. It is assumed hereinafter that

this also holds for the $Ma_{x,eff}$-lag due to other sources. The same holds for the development of the yaw velocity component $Ma_y$.

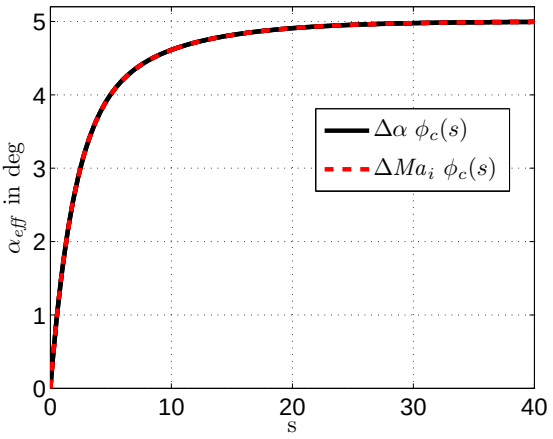


Figure 3: Effective Angle of attack using the indicial response for $\Delta\alpha$ and for $\Delta Ma_i$

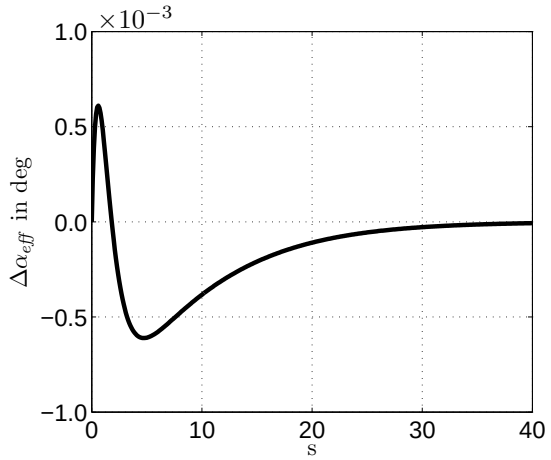


Figure 4: Deviation of effective angle of attack

Therefore, the resulting combined aerodynamic model uses the indicial circulatory lift response formulation of Beddoes and Leishman as a kind of indicial velocity response formulation for all three velocity components at the blade elements. The effective velocities are used as input for Leiss's semi-empirical analytical model. The implementation also encompasses the impulsive responses as developed by Leishman and presented in section 2.1. Stall shift is computed via the state-space representation of equation (16) that reads

$$\begin{aligned} \dot{x}_{\Delta ss} &= -\tfrac{2Ma}{T}\beta^2\, b_{os}\, x_{\Delta ss} + Ma_z(t) \\ \Delta Ma_{z,ss} &= -\tfrac{2Ma}{T}\beta^2\, b_{os} A_{os}\, x_{\Delta ss} + Ma_z(t) \end{aligned} \tag{22}$$

with $A_{os} = 1.0; b_{os} = 0.26$.

## 4. Results

The results presented in this section were generated using the combined model described in the previous sections and an already existing data set for the adapted version of Leiss's aerodynamic model of the NACA 23012 airfoil with a tabbed trailing edge. A limitation of this model is that it makes use of the same parameter set for the circulation bell curves in the positive and negative angle of attack circulation. In other words, the airfoil is treated as a symmetrical airfoil regarding the circulation. In the lower Mach number regime, deviations of the symmetric behavior occur because of the bubble burst that is only modeled for the positive angle of attack circulation.

For comparison, results for harmonic oscillations of the same airfoil using the DLR code TAU are shown. The CFD solutions were obtained within the EU-funded project SABRE [17]. Simulations were carried out for a quasi-steady case and an unsteady test case for various Mach numbers. In the quasi-steady test case, the airfoil pitched with a reduced frequency $k = \omega c/2V = 0.0005$. The unsteady test case was carried out at $k = 0.05$. Normally, this value is seen as the lower limit of the need to simulate the aerodynamics taking into account unsteady effects. Since very large amplitudes of angle of attack changes were applied in the simulations - at $Ma = 0.4$ an amplitude of $24\ deg$ was used - the changes in flow velocities at the airfoil are nevertheless quite large. Hence, the unsteady calculations show large hysteresis loops.

In Figures 5 to 7, the results of the airfoil oscillating with an amplitude of $24\ deg$ at a free stream Mach number of 0.4 are shown. In the positive angle of attack range, the steady results for the normal force coefficient are matching quite well, especially regarding the gradient for attached flow and the location of the maximum. The unsteady calculations also correspond very well in that range which means that the dynamic stall overshoot can be captured by the model. In the negative $\alpha$ range, the steady values already differ significantly. The TAU results additionally show a high frequency oscillation in the stalled region around $-15\ deg > \alpha > -20\ deg$ that is also apparent in the tangential and moment coefficient. This oscillations occur because of the unsteady flow field that develops in the detached flow, generating a high frequency variation of the airfoil parameters even at the same angle of attack. Due to the lower absolute values of the steady TAU calculations, the hysteresis in the pitch-up movement, i.e. $-24\ deg \leq \alpha \leq 0\ deg$, also exhibits lower values than the presented model. The reattachment of the flow seems to occur at the same angle of attack nevertheless.

The tangential force coefficients in Figure 6 differ significantly in the static as well as the dynamic test case. Both maxima that can be seen in the (quasi-)steady calculations are associated with the suction peaks of the attached flow circulation. In the positive stalled region of $\alpha > 13\ deg$ the static values of the model are much lower than those of the TAU calculations, i.e. a bigger rise in drag is predicted. Con-

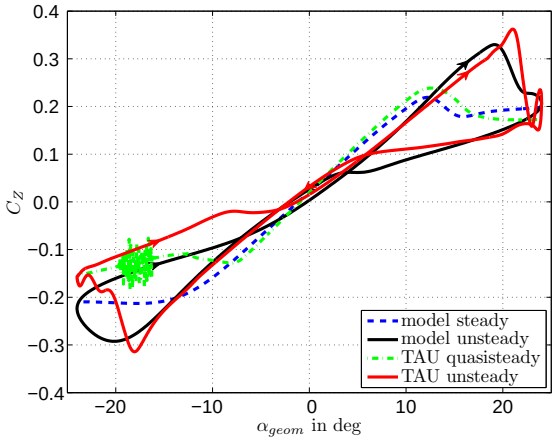


Figure 5: Normal force coefficient hysteresis for harmonically oscillating NACA 23012 at $Ma = 0.4$, $k = 0.05$, $\Delta\alpha = 24\ deg$

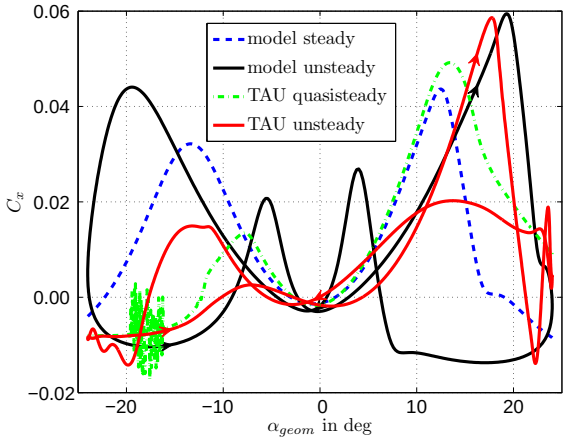


Figure 6: Tangential force coefficient hysteresis for harmonically oscillating NACA 23012 at $Ma = 0.4$, $k = 0.05$, $\Delta\alpha = 24\ deg$

sequently, the unsteady calculations of TAU yield greater tangential force coefficient values in the pitch-down movement. During pitch-up, the delay of suction peak development and the overshoot are matching quite well. In the negative angle of attack range pitch-up movement it is the other way round: the steady values are nearing each other at $\alpha < -20\ deg$. Therefore, the detached flow hystereses are closer together up to about $\alpha = -10\ deg$. For higher angles, the flow reattaches and a small suction peak occurs. This peak is much stronger with the analytical model since there, the static suction peak is also much bigger. This is due to the same modeling of the negative angle of attack circulation as for the positive angle of attack range and also causes the hysteresis loop to be much larger in the negative angle of attack pitch-down movement. The features of the hysteresis curves discussed until now suggest a similarity in the occurring flow phenomena between the calculations despite the differing absolute values. A major distinction in the behavior of the airfoil occurs during the pitch-down movement at $8\ deg > \alpha > 0\ deg$. The analytical model predicts the reattachment of the flow there - as can also be seen in Figure 5 - and consequently a suction peak, delayed with respect to the steady one, occurs. The TAU results do not show this at all.

Figure 7 shows the comparison of the pitching moment coefficients. The steady values match very well, but in the unsteady calculations the analytical model fails to predict a main feature of the curve, which is the peaks in the moment when the airfoil stalls. These peaks originate in the shedding of a vortex from the airfoil nose and its travel across the airfoil surface. When the vortex approaches the trailing edge, the load distribution over the airfoil changes significantly, which leads to the observed peaks. The vortex shedding mechanism is no part of Leiss's model and therefore is not represented in the simulation. On the other hand, the broad hysteresis that occurs in the medium angle of attack range is captured quite well and can be attributed to the

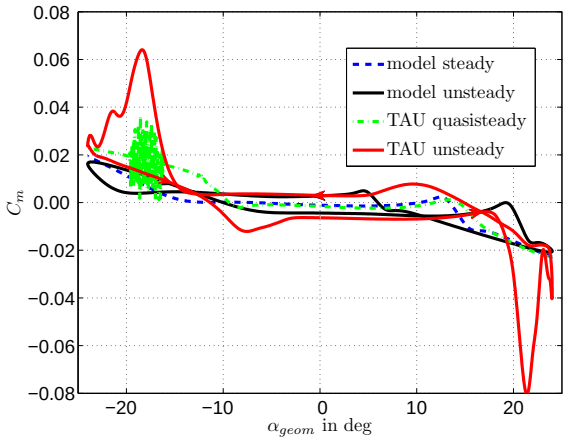


Figure 7: Pitch moment coefficient hysteresis for harmonically oscillating NACA 23012 at $Ma = 0.4$, $k = 0.05$, $\Delta\alpha = 24\ deg$

noncirculatory moments generated by the unsteady motion.

Since the steady airfoil data already differ significantly for other Mach numbers, it is more difficult to compare the airfoil behavior of the model and the CFD simulations. Therefore, instead of comparing additional hysteresis curves, a short qualitative assessment of the results is given here.

As in the $Ma = 0.4$ test case, the $C_z$ coefficients and the hysteresis behavior match quite well for other Mach numbers. For the tangential force coefficient, the additional reattachment after passage of the detached flow regime at small angles of attack also happens up until a Mach number of $0.6$. The steady airfoil values differ the most for this coefficient however, which at least partly leads to the poor match with CFD data. Because of the lack of a model for the vortex shedding, the model fails to predict the moment peaks also for other test cases. The noncirculatory effects seem to be underestimated for the moment coefficient for

the higher Mach number test cases.

## 5. CONCLUSION AND OUTLOOK

A new approach of using an indicial response formulation in conjunction with the semi-empirical analytical aerodynamics model of Leiss has been presented. This combined model was tested using an existing analytical Leiss model of the NACA 23012 airfoil in steady and harmonically oscillating test cases. The results show a good correlation with the results of TAU calculations for the normal force coefficient. The behavior of the combined model differs significantly for the tangential and pitching moment coefficient, however.

It is difficult to distinguish between the deviations due to different steady airfoil behavior and the possible adjustment needed for the unsteady airfoil behavior in the dynamic test cases. Therefore, a new analytical parameter set for the airfoil is needed that matches the steady airfoil data. Especially the assumption of the same circulation function values for positive and negative angles of attack needs to be dropped in order to enable a better fit of the data. The resulting parameter set can then be used for the re-evaluation of the prediction capabilities.

Even though the values used for the comparison are results of a higher fidelity tool, it is not clear whether the simulations capture all physical effects. Hence, the evaluation of the agreement of unsteady airfoil behavior with experimental data would be helpful to adapt the model to a realistic behavior. The usage of test cases that incorporate unsteady motion at different reduced frequencies would further aid in that.

### ACKNOWLEDGMENTS

The work presented in this paper was funded by the German Federal Ministry of Education and Research under support code 20H1506. The responsibility for the content of this paper lies with the author.

The author wishes to thank Berend G. van der Wall for his help in the understanding of the aerodynamic model of Leiss and his adaption of the model. The author would also like to thank Anthony Gardner for making available the results of the CFD calculations.

### REFERENCES

[1] van der Wall, B. G., Lim, J. W., Smith, M. J., Jung, S. N., Bailley, J., Baeder, J. D., and Boyd Jr., D. D., "The HART II International Workshop: an Assessment of the State-of-the-art in Comprehensive Code Prediction," *CEAS Aeronautical Journal*, Vol. 4, No. 3, 2013, pp. 223–252.

[2] Lomax, H., "Indicial Aerodynamics," *Manual on Aeroelasticity, Part II, Chapter 6*, edited by W. P. Jones, Technical Editing and Reproduction, London, England, 1961.

[3] Wagner, H., "Über die Entstehung des dynamischen Auftriebes von Tragflügeln," *Zeitschrift für angewandte Mathematik und Mechanik (ZAMM)*, Vol. 5, No. 1, 1925, pp. 17–35.

[4] Küssner, H. G., "Zusammenfassender Bericht über den instationären Auftrieb von Flügeln," *Luftfahrtforschung*, Vol. 13, No. 12, 1936, pp. 410–424.

[5] Jones, R. T., "The Unsteady Lift of a Wing Of Finite Aspect Ratio," *NACA TR 681*, 1940.

[6] Mazelsky, B. and Drischler, J. A., "Numerical Determination of Indicial Lift and Moment Functions for a Two-Dimensional Sinking and Pitching Airfoil at Mach Numbers 0.5 and 0.6," *NACA TN 2739*, 1952.

[7] Beddoes, T. S., "A Synthesis of Unsteady Aerodynamic Effects Including Stall Hysteresis," *Vertica*, Vol. 1, No. 2, 1976, pp. 113–123.

[8] Beddoes, T. S., "Practical Computation of Unsteady Lift," *8th European Rotorcraft Forum*, Aix-en-Provence, France, 1982.

[9] Leishman, J. G. and Beddoes, T. S., "A Generalized Model for Airfoil Unsteady Aerodynamic Behaviour and Dynamic Stall Using the Indicial Method," *42nd Annual Forum of the American Helicopter Society*, Washington D.C., June 1986.

[10] Leishman, J. G. and Crouse Jr., G. L., "A State-Space Model of Unsteady Aerodynamics in a Compressible Flow for Flutter Analyses," *27th AIAA Aerospace Sciences Meeting*, Reno, Nevada, 1989.

[11] Leiss, U. and Wagner, S., "Toward a Unified Representation of Rotor Blade Airloads With Emphasis on Unsteady and Viscous Effects," *13th European Rotorcraft Forum*, Arles, France, 1987.

[12] van der Wall, B. G., "An Analytical Model of Unsteady Profile Aerodynamics and its Application to a Rotor Simulation Program," *15th European Rotorcraft Forum*, Amsterdam, Netherlands, 1989.

[13] Schwamborn, D., Gerhold, T., and Heinrich, R., "The DLR TAU-Code: Recent Applications in Research and Industry," *ECCOMAS CFD 2006*, Egmond aan Zee, Netherlands, June 2006.

[14] Leishman, J. G., "Validation of Approximate Indicial Aerodynamic Functions for Two-Dimensional Subsonic Flow," *AIAA Journal of Aircraft*, Vol. 25, No. 10, 1988, pp. 914–922.

[15] Leiss, U., "A Consistent Mathematical Model to Simulate Steady and Unsteady Rotor-Blade Aerodynamics," *10th European Rotorcraft Forum*, The Hague, Netherlands, 1984.

[16] Leiss, U., “Unsteady Sweep - a Key to Simulation of Three-Dimensional Rotor Blade Airloads,” *11th European Rotorcraft Forum*, London, England, 1985.

[17] Rauleder, J., van der Wall, B. G., Abdelmoula, A., Komp, D., Kumar, S., Ondra, V., Titurus, B., and Woods, B. K. S., “Aerodynamic Performance of Morphing Blades and Rotor Systems,” *AHS International 74th Annual Forum and Technology Display*, Phoenix, Arizona, May 2018.